IMMOBILE WATER DETERMINATION IN SHALY SANDSTONE

B. A. Baldwin
Phillips Petroleum Co.

ABSTRACT

The production of dry hydrocarbons from low resistivity, high water saturation, formations has been previously observed and reported. Generally the model used to interpret these observations has involved modifying the mechanisms of electrical conductivity through the affected rocks. These modifications, particularly cation exchange capacity, result in new interpretations of log information in which the apparent high water saturations were reduced to more sensible values. In shaly sandstone from the Gulf Coast we found zones which have high saturation exponents ($n > 10$) and retain in excess of 80% PV water. These high immobile water saturations appear to be the result of a clay fabric which contains pores small enough to immobilize water even at high capillary pressures. Two of three successfully tested methods for estimating immobile water saturations, the porous plate and humidity cabinet, take too long to be useful for helping the field engineer with the initial interpretation of logs and deciding which zones merit production testing. Predicting immobile water saturation by NMR T1 relaxation has the advantages of being fast, transportable to field locations, and is an intrinsic measure of the mechanisms which determine the immobile water in cores with microporosity.

INTRODUCTION

Determining the amount of water present in potential production zones and the fraction that will be produced with the hydrocarbon is very important for economic, and more recently environmental, considerations. Some shaly sandstones, that have apparent high water saturations, produce dry hydrocarbons (Zemanek, 1987; Vajnar et al.,1977). Determining which zones will hold water and which will not, without expensive production testing of each zone, has been a vexing problem to production engineers for many years (Dunlap et al., 1949; Hill and Milburn, 1956; Heckel, 1985; Givens, 1987). One common model involves modifying the mechanism of electrical conduction through the rock (Givens, 1987; Waxman and Smits, 1968). These modifications result in new interpretations of the log information in which the apparent water saturations are adjusted to more sensible values.

This project proceeded chronologically in three phases. First, in response to a field request for a saturation exponent correction so that the resistivity logs would predict actual saturations, it was found that the logs were generally calculating the correct water saturations. However, some zones were immobilizing more water than the standard cutoff saturation. Second, it was necessary to determine if this was an artifact or if there was a mechanism which could produce these high immobile water saturation zones. Third, once a possible mechanism was identified and experimental artifacts ruled out, the objective changed to the development of a method for estimating immobile water saturations in shaly sandstone which would be useful to the field engineer and initial log interpretation. Ideally the method should a) be transportable to the well site or nearby field office, b) provide analysis in a few hours while the hole is still open, c) be operable by field personnel without extensive training and d) work with a variety of sample shapes and sizes.

EXPERIMENTAL

Core

Shaly sandstone core was obtained from a Gulf Coast well over two intervals. The drilling mud was a proprietary oil emulsion, made by Drilling Specialties, which contained large quantities of hematite as a weighting agent. Magnetic susceptibility measurements indicated that little, if any, hematite penetrated the core.

Initially core plugs were cut using kerosene, but fines caused plugging. Plugs with 1.5 inch diameter were successfully obtained with 26 wt. % NaCl brine. Toluene was used in a Dean-Stark extractor to remove water and oil. The plugs were then cleaned in methanol to remove the salt. Permeability and porosity were determined on the dried plugs. For NMR measurements the plugs were redrilled to 7/16 inch diameter, from the center of the 1.5 inch diameter porous plate plugs, to fit inside the Minispec NMR magnet.

Porous Plate

Porous plate desaturations were carried out simultaneously on multiple plugs using a Soil Moisture 15 Bar ceramic plate extractor. Flat areas two inches in diameter were milled into the ceramic plate to improve contact between the 1.5 inch plug and ceramic plate. The plugs were lightly polished on a fine diamond wheel to minimize irregularities at the contact face. A single ply of white unscented tissue was placed between the plate and plug and a weight was placed on top of the plug to insure good capillary contact. Desaturation was performed by applying the lowest pressure to the extractor and waiting until no more water was forced out the back side of the plate as noted on a pipet in continuous contact with the plate. The plugs were then removed, weighed, resistivity measured and replaced on the plate with a new damp tissue. The time at ambient condition was kept as short as possible and the plugs were stored in a humidified jar while measurements were being made, to minimize evaporation. With all the plugs returned to the plate the pressure was increased and the process repeated until a pressure of 190 psi was reached.

Humidity Cabinet

The Cation Exchange Capacity, CEC, test was performed in a Hotpack 434304 Temperature-Humidity Chamber (Bush and Jenkins, 1977). The test procedure consisted of weighing the samples first, after drying in a humid oven (60 C & 50% relative humidity) and second, after drying in a conventional dry oven at 110 C. CEC has been related to the amount of water absorbed on the surface by the equation

$$CEC = \text{Constant} * [1 - (\text{Unhumidified Dry wt}/\text{Humidified Dry wt})] \qquad 1)$$

where the bracketed portion is the adsorbed water index. Only the adsorbed water index will be used in this report.

NMR Relaxation

T1, spin lattice, relaxation curves were obtained with an IBM PC 20 Minispec NMR spectrometer. This instrument has a 0.47 T permanent magnet and operates at 20 MHz. The T1 relaxation curve was obtained by exciting hydrogen nuclei with an RF pulse to produce more nuclei aligned against the magnetic field (the higher energy state) than those aligned with the magnetic field (the ground state). Monitoring the strength of the resultant field as a function of time produced a T1 relaxation

curve, which by convention goes from negative to positive. Measurements at sixty four individual delay times covered the time range from .075 to 5000 ms. The rate at which the excited nuclei relax to their ground state is dependent on the local environment. Of particular interest to petroleum engineers are the effects of pore size and coatings on pore walls. In a porous media the excited hydrogen nuclei interact more strongly with the wall of a pore than with other water or oil nuclei, causing those which contact a wall to return to their unexcited state much more rapidly than those in the bulk fluid. In small pores the average distance, travel time, between individual molecules and the pore walls is smaller than in larger pores, thus the average relaxation time is shorter in smaller pores (Howard and Kenyon, 1992).

All NMR measurements were made at 100% brine saturation. The brine was 35,000 ppm NaCl in deionized water.

RESULTS AND DISCUSSION

I. Electrical measurements

Resistivity and saturation as a function of porous plate desaturation were measured on 34 plugs. Selection was made to include the range of porosity, permeability and lithology of the total core. Table 1 lists the physical and electrical properties of the 36 selected core plugs, two plugs fractured during testing. Porosity of these plugs ranged from 4 to 24%. Permeability ranged over several orders of magnitude, with the majority being less than 1 md. Formation factor values were within the range expected and a cementation factor of 1.8 was obtained for the entire group of plugs. Half of the plugs had saturation exponents (n) in the 1.5 to 2.2 range while the remainder were significantly greater than 2.2. The resistivity vs saturation plots did not show the non-linear nature often associated with conductive matrix or clay (Waxman and Smits, 1968; Givens, 1987). The saturation exponent versus immobile water plot in Fig. 1 shows that the assumption of $n=2$ would generally give reasonably correct values of water saturation up to about 80% water saturation. Higher values are not of great interest because of the small amount of available hydrocarbon, even with all the water immobilized.

II. Possible Mechanisms

In reservoir rocks, high immobile water saturations are generally associated with microporosity with high capillary pressures or heterogeneous pore structure which allows the bypassing of large quantities of water. SEM micrographs in Fig. 2, for a representative example of these shaly sandstones, show clay distributed over the rock surface. Clays, particularly chlorites, have very high surface areas and form microporous surface coatings. In addition to the small size, the pores in the clay appear to be dead ended which would prevent a significant pressure drop across these pores. The reduced pore throat size, caused by partial blocking of the sandstone pore throats with clay, may also trap additional water.

III. Possible Methods to Predict Immobile Water

Porous plate capillary pressure curves for representative plugs are shown in Fig. 3. All of the curves show a distinct break at pressures below 10 psi, thus the water saturation at pressures above 20-30 psi is close to the residual water saturation. The measured water saturation, at 190 psi, for each plug is listed in Table 1. It is important to note that at 190 psi two-thirds of these plugs contained in excess of 50% PV water; one-third were in excess of 70% PV water! The appearance of these capillary pressure curves, with the sharp break at low pressures, suggests a bimodal water storage system, one which is easily emptied at a low pressure differential and another which is not readily

desaturated. The relative amount of each storage system, in a given zone, determines the amount of water that zone would retain.

Humidity cabinet cation exchange capacity, CEC, determinations were made on all competent plugs using the humidity cabinet method developed by Core Labs (Bush and Jenkins, 1977). It should be noted that this method measures the amount of water adsorbed from a humid atmosphere onto dry rock surfaces, rather than CEC directly. The results, as a function of depth, are shown in Fig. 4. The intermediate values between the high and low points is suggestive of changes in the adsorbed water index due to lithological variations rather than random variations.

Intuitively it would seem that there should be a relationship between the sites saturated first on a dry core and those desaturated last from a wet core. The results shown in Fig. 5 indicate a correlation between the porous plate Sw at 190 psi and the adsorbed water index. This humidity cabinet method of estimating immobile saturation is quicker and easier than the porous plate desaturation method, and can measure large numbers of samples simultaneously.

If water retention is due to the presence of microporous clay fabric a correlation with other properties generally associated with the presence of clay, such as permeability, should be found. A correlation between residual water saturation, from the porous plate test at 190 psi, and permeability is shown in Fig. 6. A similar correlation was obtained between the adsorbed water index and permeability, while no significant correlations were found with porosity.

Timur (1969) used NMR relaxation measurements to predict mobile water, porosity and permeability. Zemanak (1983) used similar measurements and the assumption that water adsorbs two molecular layers thick on rock surfaces to obtain surface area measurements of core material. These suggested that NMR relaxation measurements had the potential to determine the amount of immobile water in core.

T1 relaxation experiments were run on four cores plugs for method development. The raw T1 NMR relaxation curves are shown in Fig. 7. The separation between the different cores is quite good with the core which retained the least water at the longest time, the core which retained the most water at the shortest time and the cores which retained intermediate values of water between the two extremes. The position of the rise in the curve, indicated by the time the magnetization crosses zero, is inversely correlated with the residual water, Sw at 190 psi, and the adsorbed water index, Table 2.

NMR T1 relaxation curves were obtained on seventeen additional plugs covering the observed range of water saturation after porous plate desaturation at 190 psi. Several mathematical models were fit to the NMR relaxation data in an attempt to correlate the relative amounts of immobile water. Although most of these correlations gave general trends, the scatter of data was often large. Only two methods, zero magnetization time and a stretched exponential fit (Kenyon et al. 1988), appeared to be quantitatively satisfactory and gave low data scattering. The correlation between zero magnetization time and immobile water is shown in Fig. 8. A correlation coefficient, r^2, of 0.86, where 1.0 is a perfect fit, indicates a good empirical correlation which can estimate immobile water within 10-15 %. Some of the data scatter may result from the measurement of different volumes for Sw and T1. Sw at 190 psi was determined with 1.5 inch diameter plugs while T1 was obtained with 7/16 inch diameter plugs taken from the center of the 1.5 inch plugs.

CONCLUSIONS

The log resistivity measurements in the shaly sands of the Gulf Coast appear to need no significant

correction to calculate accurate water saturations below 80% PV. However, some zones have immobile water saturations in excess of 60% PV, the standard cutoff value. Clay fabric microporosity may be responsible by trapping this water in small pores. Porous plate desaturation, humidity cabinet adsorbed water index and NMR T1 relaxation measurements all gave results which were proportional to the immobile water saturation. The porous plate desaturation takes weeks and the humidity cabinet takes days. Both require cleaning the core plugs prior to beginning the respective test. The NMR method fits the criteria for field deployment best. It a) provides a measure of the petrophysical properties which are responsible for the immobile water, b) acquires the data in less than one hour, c) allows automation of data collection and analysis on a PC, and d) is transportable to the field because the instrumentation fits on a desktop.

REFERENCES

Bush, D.C. and Jenkins, R.E., "CEC Determinations by Correlations with Adsorbed Water" SPWLA Trans. Paper H (1977).

Dunlap, H. R., Bilhartz, H.L., Shuler , E. and Bailey, C.R., "The Relation between Electrical Resistivity and Brine Saturation in Reservoir Rocks", Petrol. Trans. AIME, vol. , p259 (1949).

Heckel, B.H., "Enhanced Hydrocarbon Recognition - A New Approach to Well Evaluation for for Sand-Shale Sequences", Paper No. 85-36-45 presented at the 36th Ann. Tech. Meeting of the Petroleum Society of CIM, Edmonton, Canada, June 2-5, 1985.

Hill, H.J. and Milburn, J.D., "Effect of Clay and Water Salinity on Electrochemical Behavior of Reservoir Rocks", Petrol. Trans. AIME, Vol. 207, p65 (1956)

Howard, J.J. and Kenyon, W.E., "Determination of Pore Size Distribution in Sedimentary Rocks by Proton Nuclear Magnetic Resonance", Marine Petrol. Geol. vol. 9, p139 (1992).

Givens, W.W., "A Conductive Rock Matrix Model (CRMM) for the Analysis of Low-Contrast Resistivity Formations", The Log Analyst, Vol. 28, p 138 (1987).

W.E. Kenyon, P.I. Day, C. Straley, and J.F. Willemsen, "A Three-Part Study of NMR Longitudinal Relaxation Properties of Water-Saturated Sandstones", SPE Form. Eval. Vol. 3, pp 622-36 (1988).

Timur, A., "Pulsed Nuclear Magnetic Resonance Studies of Porosity, Movable Fluid and Permeability of Sandstones" J. Pet. Tech. vol. 21, p775 (1969).

Vajnar, E.A., Kidwell, C.M. and Haley, R.A.,"Suprising Productivity from Low-Resistivity Sands", paper EE presented at the SPWLA Eighteenth Ann. Logging Symp., June 5-8 (1977).

Waxman, M.H. and Smits, L.J.M., "Electrical Conductivities in Oil-Bearing Shaly Sands", Soc. Petro. Engr. J. 107-22 (1968).

Zemaneck, J., "Method of Locating Potential Low Water Cut Hydrocarbon Reservoirs", U.S. Patent 4,413,512 (1983).

Zemanek, J., "Low-Resistivity Hydrocarbon-Bearing Sand Reservoirs" SPE 15713 (1987).

APPENDIX

Analysis of NMR data

The T1 NMR relaxation signal is produced by exciting the hydrogen nuclei of fluids placed inside a powerful magnet with radio frequency energy, and the T1 relaxation curve is determined by monitoring the resulting change in magnetization with time. The magnetization decays in an exponential fashion. When only a single component is present, i.e. a single molecular species and a single environment, the logarithm of magnetization versus time produces a linear curve with the slope equal to the relaxation rate, reciprocal of the relaxation time, T1. Since the T1 relaxation times of the fluids in the core are dependent on pore size and surface coating, and cores typically have a range of pore sizes, the time dependence of nuclei magnetization is given by integrating over all the individual relaxation curves

$$M(t)=\int_0^i M_0(i)(1-2e^{-(\frac{t}{T1_i})})di \quad \text{.....A1}$$

M(t) is the measured magnetization as a function of time, $M_0(i)$ is the thermal equilibrium magnetization of pore size i (proportional to the number of nuclei in pore size i), t is the delay time, T1(i) is the relaxation time in pore size i and integration is over all pore sizes i. There are no unique solutions to this equation because T1(i) and $M_0(i)$ are independent variables and different distributions of pore size can give similar M(t) curves. With an exhaustive geological microscopic analysis of the core it should be possible to develop a statistical pore size distribution which would allow Eq. A1 to be solved. However, the length of time that such a study would take precludes it being useful for initial interpretation of logs.

The following discussions describe three ways of providing approximate solutions to Eq. A1. A fourth possible method of analysis (Howard and Kenyon, 1992) has been recently described, but was not used here. It's inclusion would not alter the choice of method for field application.

The simplest approximation of Eq A1 is the sum over a limited number of exponential terms. If there are a limited number of local environments, and they are the same for all the samples, this would be a very good approximation. A variety of possible combinations of exponential terms were tried to fit the four T1 relaxation curves in Fig. 7. The best fits required three or more exponential terms. However, allowing for a best fit with no restrictions made it difficult to compare the different samples. Good least squares fits were obtained for six samples, the four shaly sandstone and two Berea Sandstone plugs, by using the following equation with four exponential terms, the first two relaxation times were fixed at $T1_1$ = 0.4 ms and $T1_2$ = 8 ms. The adjustable variables were $T1_3$, $T1_4$ and the five preexponential coefficients.

$$M(t)=Ae^{-(\frac{t}{T1_1})}+Be^{-(\frac{t}{T1_2})}+Ce^{-(\frac{t}{T1_3})}+De^{-(\frac{t}{T1_4})}+E \quad \text{.....A2}$$

M(t) is the magnetization at delay time t, the four T1's are the relaxation times for the individual exponentials and the constant E was included to account for a nonzero baseline. For comparison the preexponential coefficients were normalized such that they summed to 100. The preexponential coefficients and T1 values for each of the samples are given in Table A1 and plotted in Fig. A1. Also included are two Berea Sandstone plugs, which typically desaturate to 10-15 % PV. The magnitudes of the preexponential coefficients suggest that the greater amounts of short relaxation time components are associated with the capacity to immobilize higher water saturations. These

shorter relaxation time components are indicative of water in small pores or close to a surface, such as in the clay fabric shown in Fig. 2. There could be a tendency to assign the different tau values to specific pore types or sizes, however, this could be misleading unless there is corroborating geological evidence. Although there is a reasonable qualitative correlation between immobile water and the fit to the four exponential equation, quantitative prediction of immobile water from NMR data would be difficult because both T1s and the preexponential coefficients were allowed to be variables. Attempts to use all fixed T1 values, which would make comparison between samples easier, gave much poorer fits.

The zero magnetization time method consisted of measuring the time at which the NMR T1 relaxation curve crossed zero; for examples see the curves in Fig. 7. A plot of the zero magnetization times against the logarithm of the immobile saturations, shown in Fig. 8, gives a good correlation. The time of zero magnetization and other pertinent properties are given in Table A2. Although we cannot derive a simple analytical relationship, Eq. A1 does tell us that the time when magnetization equals zero is affected by two important properties related to immobile water, pore size and the number of nuclei in the smaller pores. This empirical correlation appears to be capable of estimating the immobile water saturation within 10-15%. This technique should work anywhere microporosity causes high immobile water saturations.

The stretched exponential method (Kenyon et al., 1988) was found to estimate permeability with fewer parameters than the two or three term exponential equations. The equation is similar to Eq. A1 except it includes an additional term, alpha, in the exponent and the T1 relaxation time is termed Ts to identify it as a stretched exponential relaxation time.

$$M(t)=M_0 e^{-(\frac{t}{Ts})^{\alpha}} \qquad \text{A3}$$

This model has the advantage of varying continuously, probably more like nature, rather than in discrete steps like the fixed exponential terms in the simple summation models. The coefficients were determined using a PC SAS non-linear regression program. A better fit was obtained when the thermal equilibrium magnetization, M_0, was determined from an average at long delay times rather than as one of the variable in the regression program. The stretch relaxation time, Ts, is included in Table A3. The plot of Ts versus immobile water saturation gives a good fit as shown in Fig. A2 with a correlation coefficient, $r^2=0.81$. This indicates that the stretched exponential relaxation time could also be used to predict immobile water.

All three methods of analyzing the NMR T1 relaxation curves give good fits to the data. The summation of a few exponential terms is difficult to compare between samples unless a single set of exponentials could be used. The stretched exponential gives the most information (number of nuclei from Mo, relaxation time Ts and alpha) but requires complete T1 relaxation curves. The zero magnetization time requires the least amount of data and could be programmed with an iterative process to require as few as 7 to 9 data points. For field measurements the zero magnetization is the most productive and requires the least time. For more detailed analysis the stretched exponential method or the recently reported multiple exponential fit, using a regularization method for solution (Howard and Kenyon, 1992), can provide additional information.

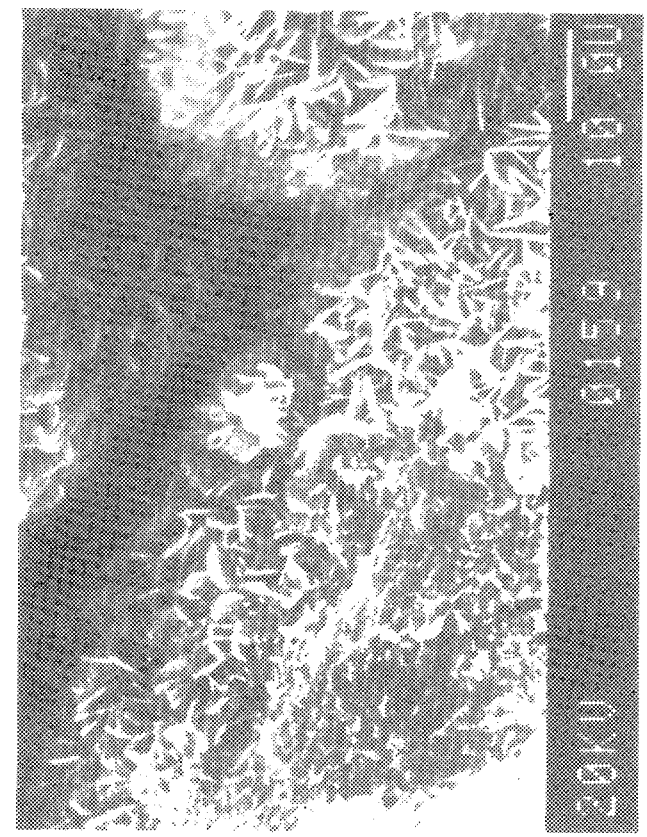

FIG. 2 MICROGRAPH OF CLAY IN SHALY SANDSTONE

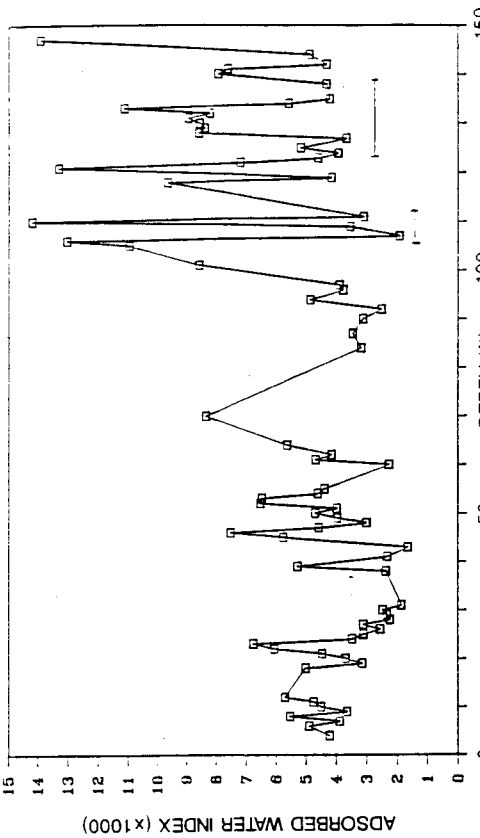

FIG. 4 ADSORBED WATER INDEX AS A FUNCTION OF DEPTH

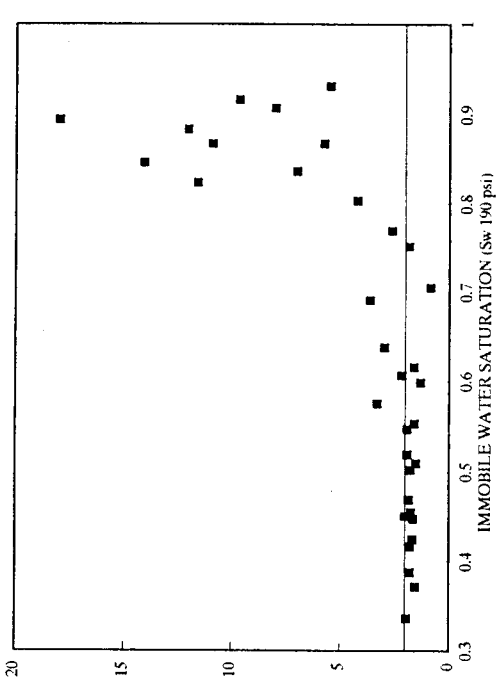

FIG. 1 SATURATION EXPONENT AND IMMOBILE WATER SATURATION

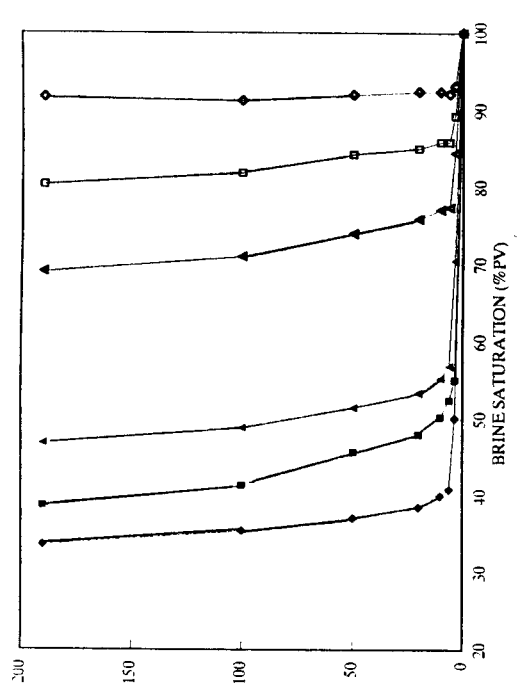

FIG. 3 POROUS PLATE CAPILLARY PRESSURE CURVES FOR SHALY SANDSTONE

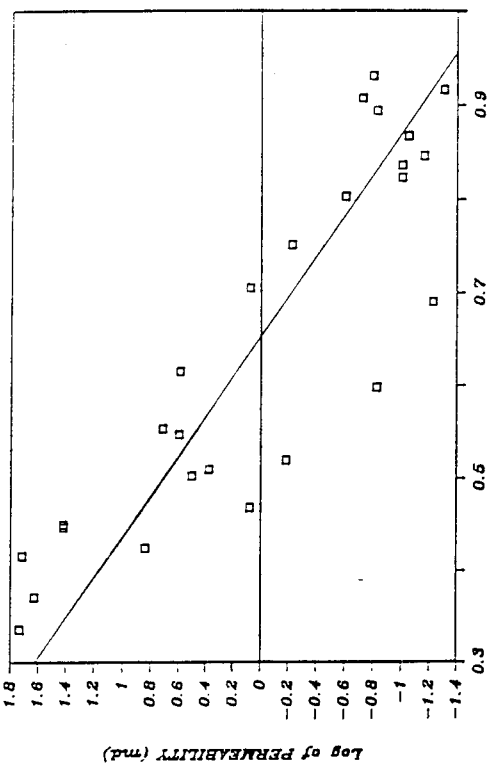

FIG. 6 CROSSPLOT OF PERMEABILITY AND IMMOBILE WATER

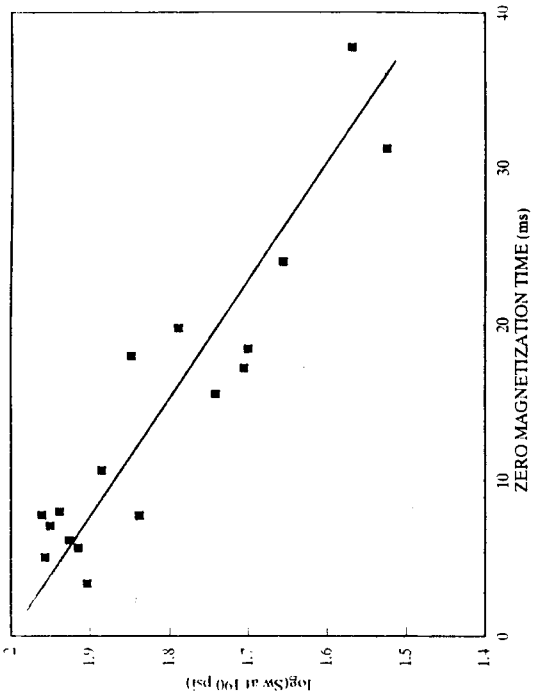

FIG. 8 CORRELATION BETWEEN ZERO MAGNETIZATION TIME AND IMMOBILE WATER

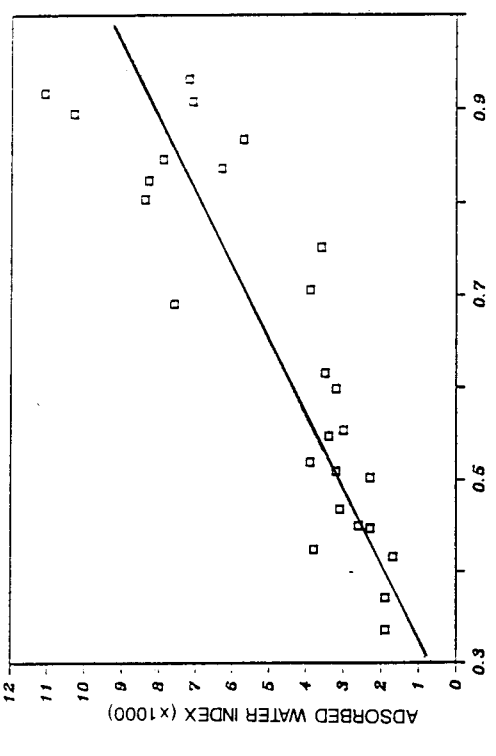

FIG. 5 CROSSPLOT OF ADSORBED WATER INDEX AND IMMOBILE WATER

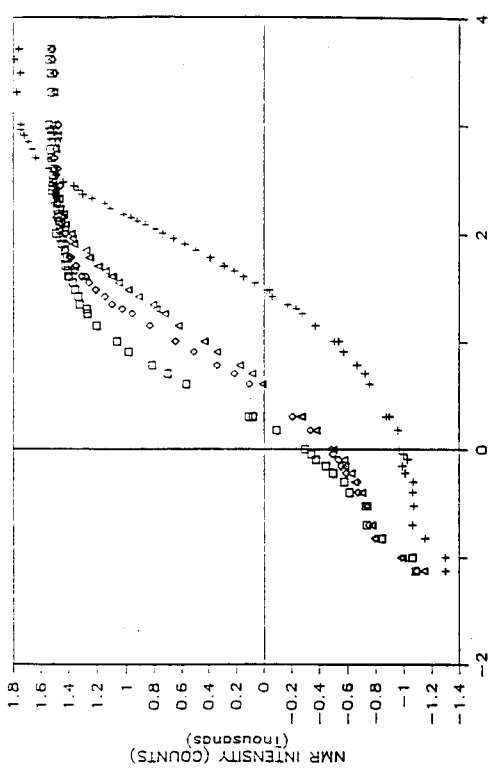

FIG. 7 T1 RELAXATION CURVES FOR CORES WITH A RANGE OF IMMOBILE WATER

APPENDIX

Analysis of NMR data

The T1 NMR relaxation signal is produced by exciting the hydrogen nuclei of fluids placed inside a powerful magnet with radio frequency energy, and the T1 relaxation curve is determined by monitoring the resulting change in magnetization with time. The magnetization decays in an exponential fashion. When only a single component is present, i.e. a single molecular species and a single environment, the logarithm of magnetization versus time produces a linear curve with the slope equal to the relaxation rate, reciprocal of the relaxation time, T1. Since the T1 relaxation times of the fluids in the core are dependent on pore size and surface coating, and cores typically have a range of pore sizes, the time dependence of nuclei magnetization is given by integrating over all the individual relaxation curves

$$M(t)=\int_0^i M_0(i)(1-2e^{-(\frac{t}{T1_i})})di \quad \text{.....A1}$$

M(t) is the measured magnetization as a function of time, $M_0(i)$ is the thermal equilibrium magnetization of pore size i (proportional to the number of nuclei in pore size i), t is the delay time, T1(i) is the relaxation time in pore size i and integration is over all pore sizes i. There are no unique solutions to this equation because T1(i) and $M_0(i)$ are independent variables and different distributions of pore size can give similar M(t) curves. With an exhaustive geological microscopic analysis of the core it should be possible to develop a statistical pore size distribution which would allow Eq. A1 to be solved. However, the length of time that such a study would take precludes it being useful for initial interpretation of logs.

The following discussions describe three ways of providing approximate solutions to Eq. A1. A fourth possible method of analysis (Howard and Kenyon, 1992) has been recently described, but was not used here. It's inclusion would not alter the choice of method for field application.

The simplest approximation of Eq A1 is the sum over a limited number of exponential terms. If there are a limited number of local environments, and they are the same for all the samples, this would be a very good approximation. A variety of possible combinations of exponential terms were tried to fit the four T1 relaxation curves in Fig. 7. The best fits required three or more exponential terms. However, allowing for a best fit with no restrictions made it difficult to compare the different samples. Good least squares fits were obtained for six samples, the four shaly sandstone and two Berea Sandstone plugs, by using the following equation with four exponential terms, the first two relaxation times were fixed at $T1_1$ = 0.4 ms and $T1_2$ = 8 ms. The adjustable variables were $T1_3$, $T1_4$ and the five preexponential coefficients.

$$M(t)=Ae^{-(\frac{t}{T1_1})}+Be^{-(\frac{t}{T1_2})}+Ce^{-(\frac{t}{T1_3})}+De^{-(\frac{t}{T1_4})}+E \quad \text{.....A2}$$

M(t) is the magnetization at delay time t, the four T1's are the relaxation times for the individual exponentials and the constant E was included to account for a nonzero baseline. For comparison the preexponential coefficients were normalized such that they summed to 100. The preexponential coefficients and T1 values for each of the samples are given in Table A1 and plotted in Fig. A1. Also included are two Berea Sandstone plugs, which typically desaturate to 10-15 % PV. The magnitudes of the preexponential coefficients suggest that the greater amounts of short relaxation time components are associated with the capacity to immobilize higher water saturations. These

shorter relaxation time components are indicative of water in small pores or close to a surface, such as in the clay fabric shown in Fig. 2. There could be a tendency to assign the different tau values to specific pore types or sizes, however, this could be misleading unless there is corroborating geological evidence. Although there is a reasonable qualitative correlation between immobile water and the fit to the four exponential equation, quantitative prediction of immobile water from NMR data would be difficult because both T1s and the preexponential coefficients were allowed to be variables. Attempts to use all fixed T1 values, which would make comparison between samples easier, gave much poorer fits.

The zero magnetization time method consisted of measuring the time at which the NMR T1 relaxation curve crossed zero; for examples see the curves in Fig. 7. A plot of the zero magnetization times against the logarithm of the immobile saturations, shown in Fig. 8, gives a good correlation. The time of zero magnetization and other pertinent properties are given in Table A2. Although we cannot derive a simple analytical relationship, Eq. A1 does tell us that the time when magnetization equals zero is affected by two important properties related to immobile water, pore size and the number of nuclei in the smaller pores. This empirical correlation appears to be capable of estimating the immobile water saturation within 10-15%. This technique should work anywhere microporosity causes high immobile water saturations.

The stretched exponential method (Kenyon et al., 1988) was found to estimate permeability with fewer parameters than the two or three term exponential equations. The equation is similar to Eq. A1 except it includes an additional term, alpha, in the exponent and the T1 relaxation time is termed Ts to identify it as a stretched exponential relaxation time.

$$M(t)=M_0 e^{-(\frac{t}{Ts})^{\alpha}} \qquad \text{A3}$$

This model has the advantage of varying continuously, probably more like nature, rather than in discrete steps like the fixed exponential terms in the simple summation models. The coefficients were determined using a PC SAS non-linear regression program. A better fit was obtained when the thermal equilibrium magnetization, M_0, was determined from an average at long delay times rather than as one of the variable in the regression program. The stretch relaxation time, Ts, is included in Table A3. The plot of Ts versus immobile water saturation gives a good fit as shown in Fig. A2 with a correlation coefficient, $r^2=0.81$. This indicates that the stretched exponential relaxation time could also be used to predict immobile water.

All three methods of analyzing the NMR T1 relaxation curves give good fits to the data. The summation of a few exponential terms is difficult to compare between samples unless a single set of exponentials could be used. The stretched exponential gives the most information (number of nuclei from Mo, relaxation time Ts and alpha) but requires complete T1 relaxation curves. The zero magnetization time requires the least amount of data and could be programmed with an iterative process to require as few as 7 to 9 data points. For field measurements the zero magnetization is the most productive and requires the least time. For more detailed analysis the stretched exponential method or the recently reported multiple exponential fit, using a regularization method for solution (Howard and Kenyon, 1992), can provide additional information.

Table A1

FIT OF T1 RELAXATION CURVES TO A FOUR EXPONENTIAL EQUATION

Sample No.	A	$T1_1$ (ms)	B	$T1_2$ (ms)	C	$T1_3$ (ms)	D	$T1_4$ (ms)
147	50.0	0.4	45.7	8.0	3.7	67.5	0.6	1560.0
148	6.2	0.4	17.8	8.0	42.6	81.3	33.4	265.0
163	20.1	0.4	56.6	8.0	14.4	32.2	8.8	32.4
166	19.0	0.4	46.6	8.0	32.4	43.4	2.0	616.5
B12	9.4	0.4	4.8	8.0	28.2	150.5	57.6	672.6
B16	7.4	0.4	13.8	8.0	37.8	58.3	40.9	218.9

Table A2

ZERO MAGNETIZATION TIMES

Sample No.	Time at 0 Magnet. ms	Sw (190 psi) (% PV)	Porosity (%)	Permeability (md)	Adsorb. Water Ind.
4	5.05	90.7	19.5	0.19	7.1
24	7.96	86.9	17.7	0.09	5.7
29	7.04	89.4	23.8	0.15	10.3
39	5.63	82.3	19.0	0.10	8.3
43	6.15	84.6	17.2	0.07	7.9
53	17.93	70.5	19.6	1.20	3.9
62	10.60	76.9	17.3	0.13	
65	17.15	50.9	16.9	2.40	3.2
70	19.71	61.5	10.2	3.90	3.5
77	37.74	37.1	17.4	42.70	1.9
92	15.50	55.3	19.3	5.20	3.0
100	18.37	50.2	20.4	3.20	2.3
134	23.99	45.4	16.6	1.81	
148	31.19	33.6	20.9	54.30	1.9
163	3.37	80.3	15.7	0.25	8.4
168	7.76	91.6	14.3	0.05	11.1
173	7.70	69.0	14.7	0.06	7.6

Table A3

FIT OF T1 RELAXATION CURVES TO A SKEWED EXPONENTIAL

Sample No.	M_0	Ts	alpha	Sw (190 psi) (%PV)
4	1268	8.53	0.417	90.7
24	1571	13.26	0.445	86.9
29	1441	12.31	0.450	89.4
39	771	12.99	0.377	82.3
43	299	18.79	0.320	84.6
53	709	31.95	0.649	70.5
62	887	16.89	0.395	76.9
65	1449	32.84	0.373	50.9
70	1447	39.58	0.395	61.5
77	1102	78.11	0.407	37.1
92	1193	28.23	0.389	55.3
100	1211	36.47	0.384	50.2
148	1760	56.84	0.403	33.6
163	1495	5.66	0.466	80.3
168	582	15.99	0.431	91.6
173	969	15.11	0.408	69.0

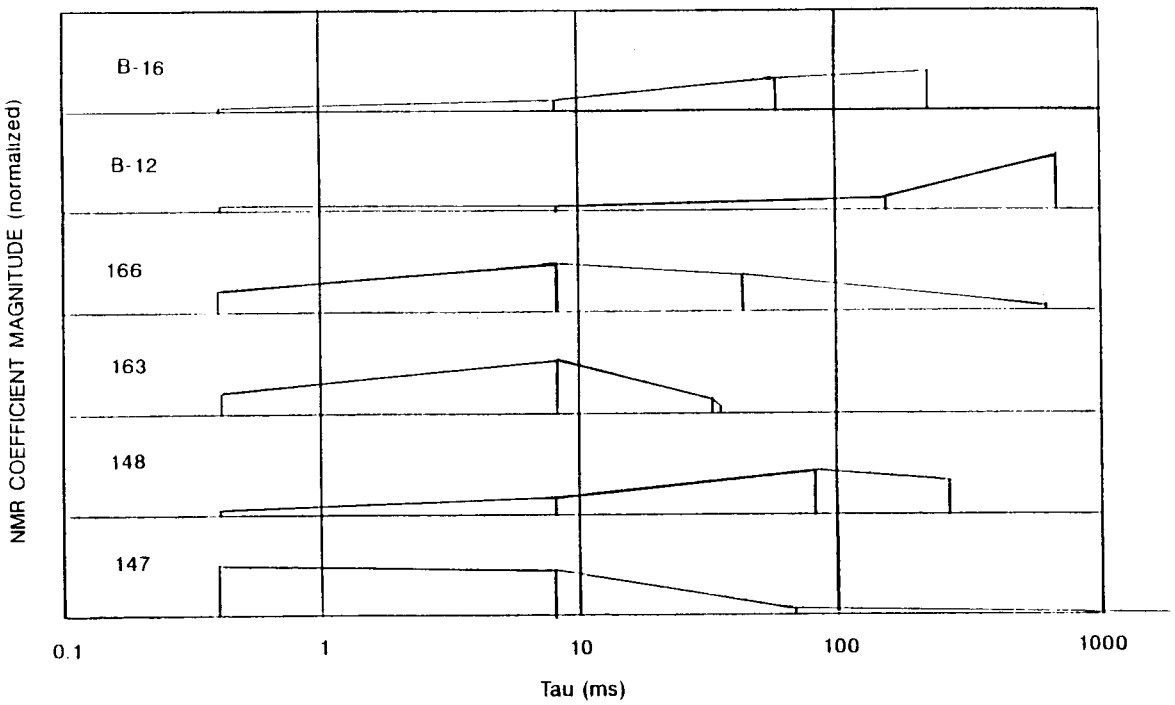

FIG. A1 RESULTS OF FITTING T1 RELAXATION CURVES TO A FOUR EXPONENTIAL EQUATION

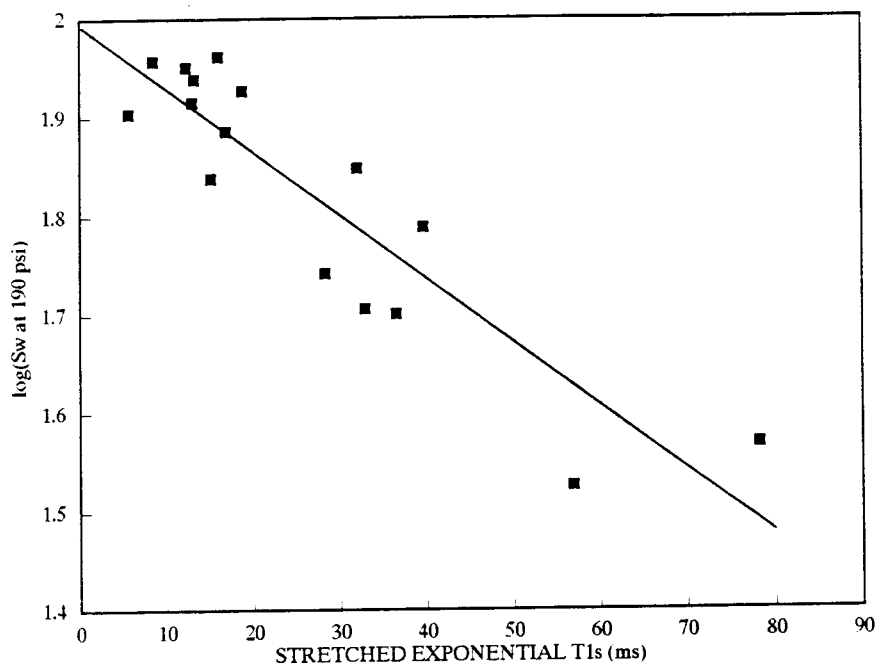

FIG. A2 CORRELATION BETWEEN STRETCHED EXPONENTIAL T1 AND IMMOBILE WATER